Jun Song, Mei Liu, Zhanping Yang*, Songwei Xu, Bowen Cheng and Pengfei Fei

Synthesis and characterization of cellulose acetate naphthoate with good ultraviolet and chemical resistance

DOI 10.1515/epoly-2016-0293
Received November 6, 2016; accepted December 28, 2016; previously published online January 20, 2017

Abstract: Commercial cellulose diacetate with a degree of substitution (DS) of 2.45 was partly deacetylated to cellulose acetate (CA) with different DSs by acid-catalyzed hydrolysis and then reacted with 1-naphthoyl chloride (NpCl) to synthesize CA naphthoate (CANp). Fourier transform infrared and ^{1}H-NMR were used to characterize the chemical structure of CANp. The DS of naphthoate moiety (DS_{CANp}) could be varied from 0.18 to 0.98 by adjusting the molar ratio of –OH in CA unit to NpCl, the DS of CA (DS_{CA}), and the reaction time and temperature. When DS_{CA} was 2.01 and the molar ratio was 1 : 6, the maximum DS_{CANp} of the product was achieved after a reaction at 80°C for 2 h. With the increase of DS_{CANp}, the thermal stability decreased slightly whereas the anti-ultraviolet property was enhanced. Moreover, the obtained films containing CANp exhibited good ultraviolet resistance as well as chemical resistance.

Keywords: cellulose acetate; chemical resistance; naphthalene moiety; thermal stability; ultraviolet resistance.

1 Introduction

Cellulose acetate (CA) prepared by acetylating cellulose is one of the most important cellulose derivatives. Because of its wide range of desirable properties (1–3), it has been used in modern coating, controlled release, optical film, and membrane as well as traditional textile fields in the forms of fiber, film, and plastic (4–6). However, it is still very essential to modify CA for its wider applications considering its weaknesses such as poor chemical resistance, low mechanical strength, low thermal resistance, compaction phenomena, and poor ultraviolet (UV) resistance (7–13). As we all know, cellulose acetate is readily dissolved under acid or alkaline environments, thus greatly limiting its applications. In view of this, many scholars devote themselves to overcoming the poor chemical resistance. For example, Liu et al. (14) blended chitosan (CS) into CA to prepare CA-CS membranes for improving the acid-base range to be consistent with the content of chitosan. By contrast, UV irradiation has been known as one of the most frequent abiotic reactions in the natural environment, and it can cause damages to organic materials like plastics, woods, or polymers in some products (15, 16). Direct exposure of the materials to climatic conditions of sunlight may significantly decrease the lifetime of these products. Hence, much effort has been attempted to improve the UV resistance of CA. Typically, metal oxide nanoparticles such as TiO_2, ZnO, ZnS, and CeO_2 can be blended into CA to obtain hybrid nanocomposites with UV-absorbing property (17, 18). However, these nanoparticles may induce photodegradation because of their photocatalytic activity (16). Jahan et al. (19), considering the noncatalytic property and good absorbance for UV radiation of graphene oxide, embedded graphene oxide into CA matrix to form a CA/graphene oxide nanocomposite film for improving the UV resistance of CA (20). Unfortunately, similar to most nanoparticles blended with polymers, graphene oxide is prone to falling off.

As one of the most important industry polycyclic aromatic hydrocarbons, naphthalene is commonly used in the synthesis of phthalic anhydride, dye intermediates, rubber additives, and pesticides. Naphthalene belongs to a photosensitive group and can be incorporated into polymer chains for good applications in photovoltaic components (21, 22). Meanwhile, naphthalene is a bicyclic aromatic molecule with six-membered ring, and the polymer containing naphthalene can possess good chemical resistance because of its lower ring strain (23–25). In addition, introducing naphthalene nucleus, which is chromophorics, into cellulose acetate chains is beneficial

***Corresponding author: Zhanping Yang,** Nantong Cellulose Fibers Co., LTD, No.109, Zhongxiu middle road, Nantong, Jiangsu 226000, China, e-mail: wallaceyang@ncfcinfo.com
Jun Song: School of Material Science and Engineering, Tianjin Polytechnic University, Tianjin, China; and Nantong Cellulose Fibers Co., Ltd., Nantong, China
Mei Liu, Bowen Cheng and Pengfei Fei: School of Material Science and Engineering, Tianjin Polytechnic University, Tianjin, China
Songwei Xu: Nantong Cellulose Fibers Co., Ltd., Nantong, China

to the absorption of UV light (26, 27). However, to the best of our knowledge, previous research has seldom focused on improving CA characteristics by incorporating naphthalene moiety.

In this paper, commercial cellulose diacetate (CDA) was partly deacetylated to CA with different degrees of substitution (DSs) by acid-catalyzed hydrolysis. Then cellulose acetate naphthoates (CANps) with different DS_{CANp} were synthesized homogeneously in pyridine. The chemical structures of CANps were characterized, and their thermal property and UV resistance were evaluated. Finally, the films containing CANp with good UV and chemical resistance were successfully prepared.

2 Materials and methods

2.1 Materials

Cellulose diacetate (CDA) with a DS of 2.45, supplied by Nantong Cellulose Fibers Co., Ltd., was dried to less than 1% moisture before use. 1-Naphthoyl chloride (NpCl) (>99%) was purchased from Aladdin Reagent Co., Ltd. Pyridine was distilled under reduced pressure and stored over molecular sieves. N,N-dimethylformamide (DMF), ethanol (EtOH), glacial acetic acid (HAc), concentrated sulfuric acid (H_2SO_4), anhydrous sodium acetate (CH_3COONa), sodium hydroxide (NaOH), and hydrochloric acid (HCl) were obtained from Kermel Chemical Co., Ltd. All reagents were analytically pure and used without further purification.

2.2 Preparation of CA with different DSs through hydrolysis

CDA (3.0 g) and HAc (13.5 g) were mixed in a 100-ml round bottom flask with a reflux condenser. The mixture was heated to 60°C under continuous agitation in an oil bath and preserved for 20 min to dissolve CDA. Then 0.24 g of H_2SO_4 and 1.2 g of water were successively added dropwise to the flask to avoid degradation of CDA and precipitation phenomenon. After several hours (2, 4, 6, 8, and 12 h), a proper amount of CH_3COONa was respectively added to terminate the reaction. The mixtures were separated by precipitating using excess deionized water and then filtered and washed repeatedly until neutral. Afterward, the precipitates were dried under vacuum at 60°C for 24 h. The DS_{CA} was determined according to standard ASTM D 871-96.

2.3 Synthesis of CANp

One gram of CA was dissolved in 15 g of pyridine with constant mechanical stirring at 80°C in an oil bath. Then NpCl was added proportionally to trigger the reaction. After 2 h, the reaction solution was poured into 200 ml of EtOH to cause the formation of precipitates. The precipitates were collected by filtration and then washed sequentially with EtOH (2×100 ml) and distilled water (2×100 ml). After that, the precipitates were purified by Soxhlet extraction with EtOH for 24 h. Finally, the product was dried under vacuum at 80°C for 12 h.

2.4 Fabrication of CDA, CANp, and CANp/CDA films

The films were prepared by solution casting. CANp (4 wt%) (DS_{CANp} = 0.42) and CDA (11 wt%) were dissolved in DMF by vigorous stirring at room temperature until a clear and homogeneous solution was obtained. After standing degassing for 4 h, the solution was cast on a dry, smooth glass plate using a cast knife open at 500 μm. The glass plate was then immersed in ice water bath so that the solution was coagulated to form films. The films were peeled off from the substrate and freeze-dried to remove any residual solvent. For comparison, pure CANp and CDA films were also prepared by the same way.

2.5 Chemical resistance test

Chemical resistance of the film was determined by weight loss (%) resulting from the contact between the film and the acid or alkali of a certain concentration. Preweighed CDA, CANp/CDA, and CANp films were immersed in HCl solution of 5 mol/l for 6 h and NaOH solution of 1 mol/l for 1 h sequentially, and then weighed again at room temperature. The weight loss can be calculated using the following equation:

$$\text{Weight loss}(\%) = 1 - \frac{W_c}{W_i} \times 100$$

where W_i is the weight (g) of the film before contact with solvents, and W_c is the weight after contact.

2.6 Characterization

The molecular weights were determined on a VISCOTEK270 gel permeation chromatograph (GPC, mobile phase: tetrahydrofuran (THF); concentration: 4 mg/ml).

Fourier transform infrared (FTIR) spectra were recorded with a Bruker TENSOR37 FTIR spectrometer (Bruker Optics, Ettlingen, Germany) from 4000 to 400 cm^{-1} using the KBr pellet technique.

^{1}H-NMR spectra were obtained from a Bruker-AV 400 spectrometer (Bruker Optics, Ettlingen, Germany) (500 MHz, TMS as internal standard, room temperature, solvent: DMSO-d_6). The DS_{CANp} values can be calculated from the following formula:

$$DS_{CANp} = \frac{I_{NP} \times 7}{I_{AGU} \times 7}$$

where I_{NP} and I_{AGU} denote the hydrogen peak areas of naphthoate moiety and CA unit, respectively.

Differential scanning calorimetry (DSC) was performed on NETZSH DSC 204 F1 Phoenix® (NETZSCH-Gerätebau GmbH, Selb, Germany) at a heating rate of 10°C/min in a temperature range of 20–300°C under nitrogen atmosphere. Thermogravimetric analysis (TGA) was performed on a TGA Q5000 IR thermogravimetric analyzer (TA Instruments Co. Ltd., USA) at a heating rate of 10°C/min from 20°C to 600°C under nitrogen atmosphere.

UV-Vis spectra were recorded by a Perkin Elmer Lambda35 UV-Vis spectrophotometer (Olympus Optical Co. Ltd., Japan) (200–400 nm; solvent: THF; concentration: 100 mg/l).

Tensile strength of the films was measured with an LLY-06E/PC electronic monofilament strength tester (Lai Zhou Electron Instrument Co. Ltd., Shandong, China) at room temperature. Rectangular samples (20 mm×10 mm) were prepared from each film and then measured with a gauge length of 10 mm at an extension speed of 10 mm/min.

3 Results and discussion

3.1 Hydrolysis

Cellulose and its derivatives can be functionalized by chemical reaction at the –OH groups. However, up to now, products and their property design by chemical modification are limited to certain esters and ethers, especially for CA. It is noted that there are only a low number of –OH groups in CDA so that it is difficult for CDA to react with other reagents. Hence, CDA is often modified through hydrolysis to endow it with higher reactivity and thus realize property improvement.

The main purpose of hydrolysis, including acid hydrolysis and alkaline hydrolysis (28), is to remove acetyl groups from CDA, thereby obtaining CA with different DSs. However, the products through alkaline hydrolysis cannot dissolve in conventional solvents completely because of the heterogeneous reaction that may lead to uneven distribution of substituents, which is adverse to cellulose acetate modification. Fortunately, these defects can be reduced considerably by acid hydrolysis, which is a homogeneous reaction process. In this study, acid hydrolysis process was adopted, and CA with different DSs was prepared by altering hydrolysis time given other conditions unchanged. As shown in Figure 1, the DS of CA (DS_{CA}) in the range from 2.33 to 2.00 can be achieved through the acid hydrolysis process. The DS_{CA} of hydrolyzed CA samples was determined by titration and then plotted against the reaction time. As can be seen, the DS_{CA} decreases from 2.33 to 2.01 during the reaction time 2–8 h and then shows no significant decrease with further extension of reaction time to 12 h. This is probably due to the formation of HAc during the reaction, which reduced the concentration of concentrated sulfuric acid and thus decreased the reaction rate. These results are economically favorable because this process decreases energy cost and saves reaction time. In addition, it is essential to reduce reaction time because low DS values can generate products with more potential for degradation (29).

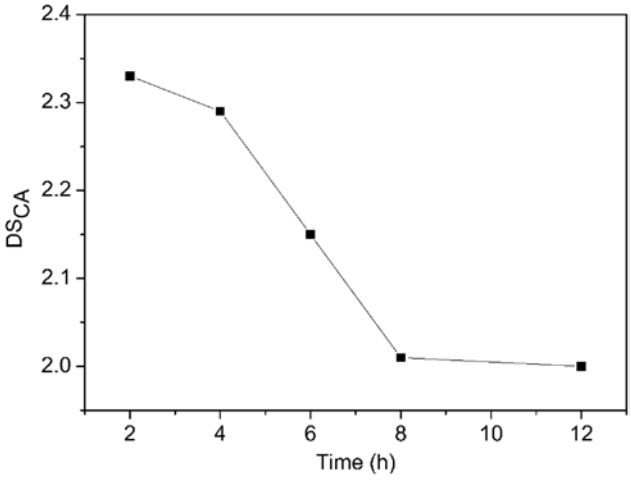

Figure 1: A relationship between DS_{CA} of hydrolysis time.

The molecular weights of CAs with different DS_{CA} by hydrolysis were measured with GPC. The results given in

Table 1: The molecular weights of different DS_{CA} cellulose acetate.

DS_{CA}	2.45	2.33	2.29	2.15	2.01	2.00
$\bar{M}n$	16,222	14,625	14,315	11,753	8557	5827
$\bar{M}w$	79,282	73,944	68,297	45,778	33,053	18,623
$\bar{M}w/\bar{M}n$	4.887	5.056	4.771	3.895	3.863	3.196

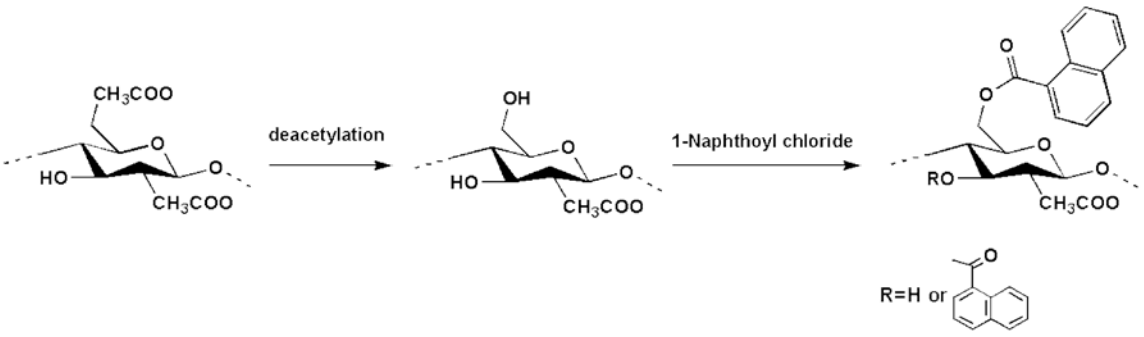

Figure 2: The synthesis route of CANp.

Table 2: Conditions and results of homogeneous reaction of CA with NpCl.

No.			Reaction conditions		
	DS_{CA}	Molar ratio[a]	Time (h)	Temperature (°C)	DS_{CANp} ^{1}H-NMR
A1	2.45	1 : 2	2	80	0.18
A2	2.45	1 : 4	2	80	0.34
A3	2.45	1 : 6	2	80	0.42
A4	2.45	1 : 6	1	80	0.30
A5	2.45	1 : 6	3	80	0.44
A6	2.45	1 : 6	2	70	0.33
A7	2.45	1 : 6	2	90	0.39
A8	2.15	1 : 2	2	80	0.57
A9	2.15	1 : 4	2	80	0.67
A10	2.15	1 : 6	2	80	0.70
A11	2.01	1 : 2	2	80	0.64
A12	2.01	1 : 4	2	80	0.97
A13	2.01	1 : 6	2	80	0.98

[a]Molar ratio of –OH of CA unit to NpCl.

Table 1 show that M_n and M_w all decrease with the decrease of DS_{CA} values. It's worth noting that the degradation phenomenon was serious especially for the DS_{CA} value of 2.00 that hydrolyzed for 12 h.

3.2 Synthesis

Esterification of CAs (DS_{CA} = 2.45 ~ 2.01) with NpCl can produce CANp with DS_{CANp} from 0.18 to 0.98. The synthetic route is illustrated in Figure 2, and detailed reaction conditions and results are given in Table 2. For samples A1–A3, the molar ratio of –OH groups in CA unit to NpCl varied from 1 : 2 to 1 : 6, and the DS_{CANp} of the products increased from 0.18 to 0.42. For samples A8–A10 and A11–A13, the esterification of CAs with different DS_{CA} values was conducted under the same reaction conditions, and their DS_{CANp} showed the similar increase trend. These results indicate that the DS_{CANp} of CANps increases with the decrease of the molar ratio of –OH groups in CA unit to NpCl and finally reaches a maximum DS_{CANp} at the molar ratio of 1 : 6. This increase is probably due to the greater availability of 1-naphthoyl ions with higher concentrations in the proximity of CAs. In addition, by comparing the DS_{CANp} of A3, A10, and A13, which were synthesized under the same conditions except for the initial DS_{CA}, it can be observed that higher DS_{CA} can further inhibit the esterification and thus lower the DS_{CANp} of the products. This phenomenon can be attributed to the decrease of the amount of active hydroxyl as well as the increase of stereo-hindrance of –OH from the high number of acetate groups.

The effects of reaction temperature and time on the DS_{CANp} values were also investigated in this study. For samples A4, A3, and A5, with the increase of reaction time, the DS_{CANp} value increased from 0.30 to 0.44 because prolonging reaction time resulted in favorable effect on the diffusion of reactants, thereby inducing better contact between etherifying agent and CA (29, 30). For samples A6, A3, and A7, the DS_{CANp} value firstly increased from 0.33 to 0.42 with the increase of reaction temperature from 70°C to 80°C, and then decreased to 0.39 with further temperature increase to 90°C. The enhancement of esterification by raising temperature is probably due to the favorable effect of temperature on compatibility of reaction ingredients (31). However, owing to the hydrolysis mechanism (32), the observed DS_{CANp} presents a slight decrease at 90°C.

3.3 Structural characterization

Figure 3 shows the FTIR spectra of CA and CANp. As can be seen in the spectra of all CANp samples, the peaks at 3475 and 2954 cm^{-1} are attributed to the absorption of –OH and C–H stretching vibrations, respectively, and the peak at 1749 cm^{-1} corresponds to the C=O stretching band

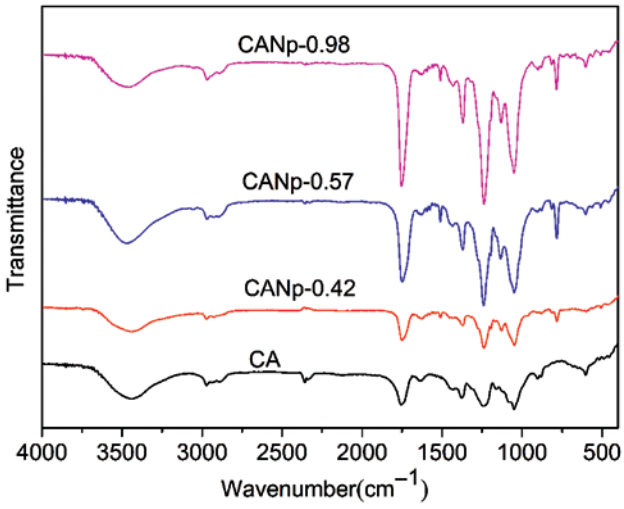

Figure 3: FTIR spectra of CA and CANp.

of the ester carbonyl group. Because the carbonyl peak of the resultant acyl naphthalene is overlapped with that of original acetyl, there is only one carbonyl absorption peak in the spectra. Moreover, the peak intensity of C=O stretching band increases with increase of DS_{CANp}. Compared with the spectrum of CA, typical signals of naphthalene appear at 1593, 1576, and 1512 cm^{-1} (24, 33). Furthermore, the absorption band at 783 cm^{-1} is related to C–H wagging vibrations of naphthalene ring. Other characteristic peaks are quite similar to those of CA (34). These results indicate that NpCl smoothly reacted with CA.

To further confirm the structure of CANp, ^{1}H-NMR spectroscopy was conducted on a sample dissolved in DMSO-d_6, and the results are shown in Figure 4. As can be seen, the chemical shifts in the range between 3.5 and 5.5 ppm are attributed to the protons (H-1 ~ H-6) of cellulose acetate backbone in the spectrum of CANp, which has the same chemical shifts as that of CA, and the peaks in the range between 7.2 and 8.8 ppm can be assigned to the naphthalene protons (H-9 ~ H-15) of CANp. These results further confirm that CA-mixed esters have been successfully synthesized.

3.4 Thermal stability

The thermal stabilities of pure CDA and CANp were measured by DSC and TGA. As Figure 5A shows, the melting temperature (T_m) of CANp decreases obviously relative to that of pure CDA, indicating that the introduction of naphthoic acid groups into cellulose acetate backbone weakens the strength of its inter- and intramolecular hydrogen bond. By contrast, the introduction of naphthalene with bulky structures is conducive to improving the thermal property by increasing the crosslinking density of polymers (33, 35). As a result, the T_m of CANp decreases slightly with the increase of DS_{CANp}. By contrast, the introduction of naphthalene has no significant effect on the mechanical property of CANp films, which can be confirmed by the UV resistance test results before exposure to UV light.

Figure 5B displays the TGA curves of pure CDA and CANp. It can be found that the onset decomposition temperature of CANp with different DS_{CANp} of 0.42 and 0.98

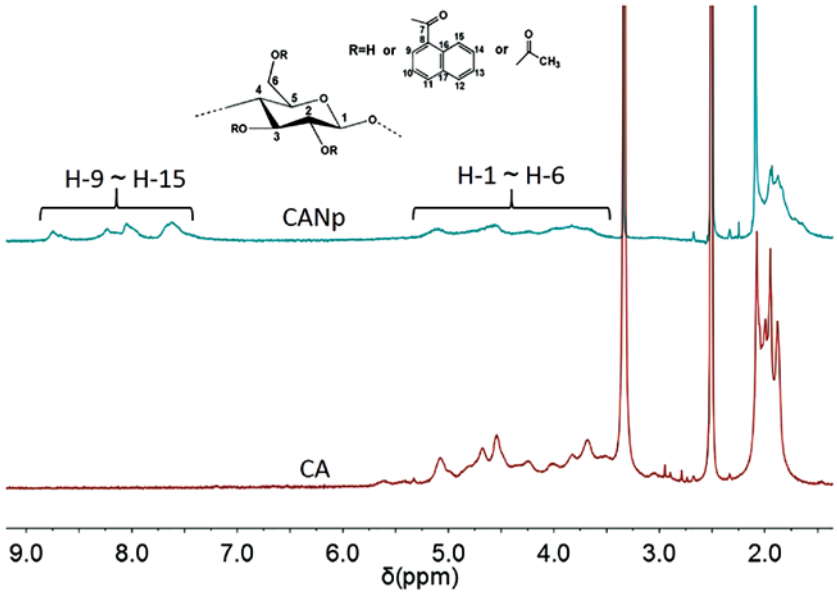

Figure 4: ^{1}H-NMR spectra of CA and CANp (CANp-0.57).

occurs at 295°C and 312°C, respectively, a little lower than the onset decomposition temperature of CDA (316°C). These results demonstrate that the thermal stability of CANp decreases to some extent compared to that of unmodified CA.

3.5 UV resistance

The anti-UV property of CANp was investigated through UV-Vis absorption spectra, as Figure 6 shows. The absorption peaks at 245, 298, and 324 nm are similar to those of naphthalene (36–38). The increase of the naphthalene substituent from 0.42 to 0.98 results in a sharp increase of absorbance at 298 nm from 1.39 to 2.67. It can be concluded that the anti-UV property of CANp is significantly improved with the increase of DS_{CANp}.

Common polymers always undergo losses in mechanical strength when exposed to UV light (39). Hence, the UV resistance of CDA, CANp/CDA, and CANp films can also be evaluated via the variation of tensile strength using UV lamps (400 W, 200–400 nm) equipped in a lab-made box. The samples were fixed at the same position in the box for 0, 2, 4, 6, and 8 days, respectively. After exposure for preset time duration, the samples were removed from UV lamps, and their mechanical properties were tested. Figure 7 shows the effect of UV exposure time on the tensile strength of CDA, CANp/CDA, and CANp films. Obviously, pure CDA film is very vulnerable to UV light, and its tensile strength decreases approximately from 2.4 to 0.8 MPa after an 8-day irradiation. By contrast, the tensile strength of pure CANp film remains almost unchanged while CANp/CDA film also decreases after UV exposure. These results suggest that naphthalene moiety

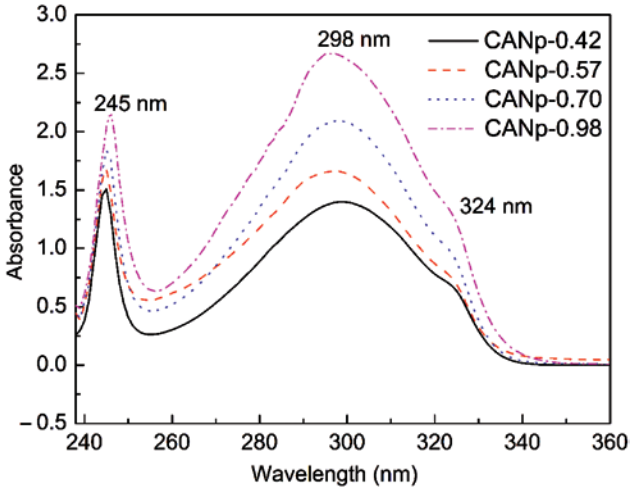

Figure 6: UV-Vis absorption spectra of CANp (concentration of CANp in THF: 100 mg/l).

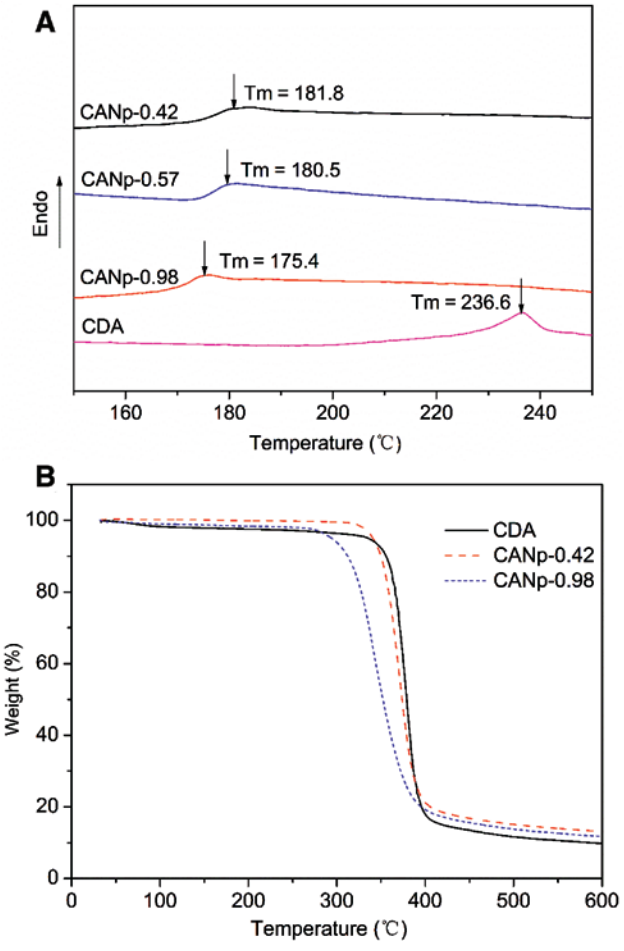

Figure 5: DSC curves (A) and TGA curves (B) of CANp.

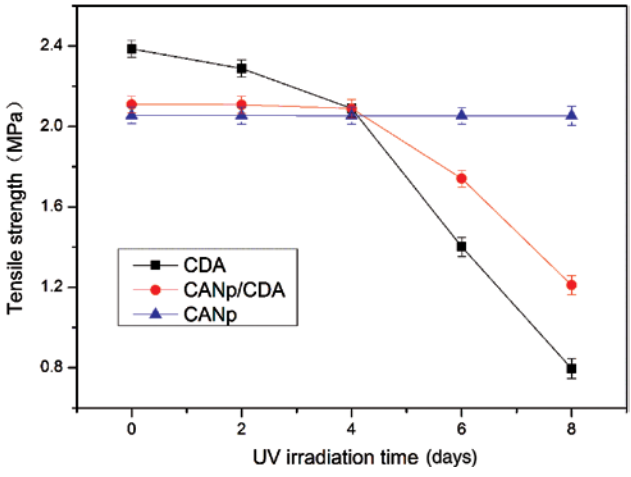

Figure 7: A correlation of tensile strength of CDA, CANp/CDA and CANp films versus the UV irradiation time.

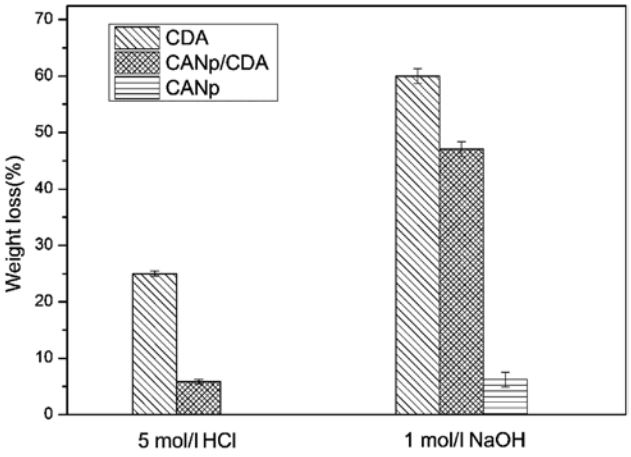

Figure 8: Chemical resistance of CDA, CANp/CDA, and CANp films in 5 mol/l HCl and 1 mol/l NaOH solutions.

in cellulose acetate molecules is considerably effective for improving the UV resistance of films.

3.6 Chemical resistance

Figure 8 shows the weight loss (%) of CDA, CANp/CDA, and CANp films after immersion in HCl and NaOH solutions for preset time duration. As can be seen, there is no weight loss (%) in HCl solution for CANp film, and its weight loss (%) in NaOH solution is approximately 6.25%; CANp/CDA film shows a measurable weight loss of 5.88% and 47.06% in HCl and NaOH solutions, respectively; by contrast, the weight loss of CDA film reaches up to 25% and 60% in HCl and NaOH solutions, respectively. These results mean that naphthalene ring groups that possess space shielding effect can hinder the attack to ester groups from the acid or alkaline medium (23, 40), thus enhancing the chemical resistance of films. It is hopeful that such good chemical resistance of CANp films can expand its application fields.

4 Conclusions

In summary, CAs with different DSs were prepared by partial acid-catalyzed hydrolysis, and CANps were successfully synthesized by homogeneous reaction with NpCl in pyridine. The chemical structures of CA-mixed esters were characterized by FTIR and ^{1}H-NMR, and the DS_{CANp} was controlled by altering the reaction parameters such as the molar ratio of reactants, the DS of CA, and the reaction time and temperature. According to the DSC, TGA, and UV-Vis results, the thermal stability of CANp was just mildly decreased, but the mechanical strength of CANp was not remarkably affected, whereas the anti-UV property was improved significantly. Meanwhile, the prepared films containing CANp were endowed with good UV and chemical resistance. The novel CA-mixed ester synthesized in this study can potentially be used in textiles, medicines, plastic films, and filtration industries, which will greatly broaden the application fields of CA materials.

Acknowledgments: The authors are thankful to the financial support from Nantong Cellulose Fibers Co., Ltd. (No. R-CNC162017).

References

1. Edgar KJ. Cellulose esters, organic. Encyclopedia of Polymer Science and Technology. 2nd ed. New York: John Wiley & Sons Inc; 2004. 129–58 p.
2. Rustemeyer P. History of CA and evolution of the markets. Macromol Symp. 2004;208:1–6.
3. Klemm D, Heublein B, Fink HP, Bohn A. Cellulose: fascinating biopolymer and sustainable raw material. Angew Chem Int Edit. 2005;44:3358–93.
4. Edgar KJ, Buchanan CM, Debenham JS, Rundquist PA, Seiler BD, Shelton MC, Tindall D. Advances in cellulose ester performance and application. Prog Polym Sci. 2001;26:1605–88.
5. Son WK, Youk JH, Park WH. Antimicrobial cellulose acetate nanofibers containing silver nanoparticles. Carbohyd Polym. 2006;65:430–4.
6. Buchanan CM, Gardner RM, Komarek RJ. Aerobic biodegradation of cellulose acetate. J Appl Polym Sci. 1993;47:1709–19.
7. Luan Y, Wu J, Zhan M, Zhang J, Zhang J. "One pot" homogeneous synthesis of thermoplastic cellulose acetate-graft-poly (l-lactide) copolymers from unmodified cellulose. Cellulose. 2013;20:327–37.
8. Routray C, Tosh B. Controlled grafting of MMA onto cellulose and cellulose acetate. Cellulose. 2012;19:2115–39.
9. Teramoto Y, Nishio Y. Biodegradable cellulose diacetate-g raft-poly (l-lactide) s: thermal treatment effect on the development of supramolecular structures. Biomacromolecules. 2004;5: 397–406.
10. Yoshikuni T, Shoko A, Tomokazu H, Yoshiyuki N. Cellulose acetate-graft-poly (hydroxyalkanoate) s: synthesis and dependence of the thermal properties on copolymer composition. Macromol Chem Phys. 2004;205:1904–15.
11. Teramoto Y, Yoshioka M, Shiraishi N, Nishio Y. Plasticization of cellulose diacetate by graft copolymerization of ε-caprolactone and lactic acid. J Appl polym Sci. 2002;84:2621–8.
12. Boday DJ, Kuczynski J. Flame retardant cellulose acetate. USA Patents; 2015.
13. Schlufter K, Schmauder HP, Dorn S, Heinze T. Efficient homogeneous chemical modification of bacterial cellulose in the ionic liquid 1-N-Butyl-3-methylimidazolium chloride. Macromol Rapid Commun. 2006;27:1670–6.

14. Liu D, Fu D, Yang Z, Zhang J. Study on preparation and properties of cellulose acetate-chitosan composite membrane. New Chemical Material. 2008;10:028.
15. Murphy SP, Moody CD. Membranes: deterioration of cellulose acetate by iron salts, oxygen, and organics. Ultrapure Water. 1997;14:19–22.
16. Calvo ME, Castro Smirnov JR, Míguez H. Novel approaches to flexible visible transparent hybrid films for ultraviolet protection. J Polym Sci Part B: Polym Phys. 2012;50:945–56.
17. Cui H, Zayat M, Parejo P, Levy D. Highly efficient inorganic transparent UV-protective thin-film coating by low temperature sol-gel procedure for application on heat-sensitive substrates. Adv Mater. 2008;20:65–8.
18. Parlak O, Demir MM. Toward transparent nanocomposites based on polystyrene matrix and PMMA-grafted CeO_2 nanoparticles. ACS Appl Mater Interfaces. 2011;3:4306–14.
19. Jahan N, Khan W, Azam A, Naqvi AH. Fabrication of transparent cellulose acetate/graphene oxide nanocomposite film for UV shielding. Aip Conf Proc. 2016;1731:228–40.
20. Singh RP, Tomer NS, Bhadraiah SV. Photo-oxidation studies on polyurethane coating: effect of additives on yellowing of polyurethane. Polym Degrad Stab. 2001;73:443–6.
21. Spies C, Lorenc A, Gehrke R, Kricheldorf HR. Fluorescence of copoly(ester-imide)s containing 2,6-naphthoate units. Macromol Chem Phys. 2003;204:813–22.
22. Köpplmayr T, Cardinale M, Jakopic G, Trimmel G, Kern W. Photosensitive polymers bearing fully aromatic esters for multilayer data storage devices. J Mater Chem. 2011;21:2965–73.
23. Mittal KL. Polyimides: synthesis, characterization, and applications. 1st ed. New York: Plenum Press; 1984.
24. Ozturk RT, Apohan NK, Gungor A. Synthesis and characterization of novel polyimides based on 2, 6-bis (m-amino phenoxy) benzoyl naphthalene. Chem Eng Trans. 2013;32:1681–6.
25. Sawai T, Wakabayashi K, Yamazaki S, Uchida T, Sakaguchi Y. Synthesis and morphology control of self-condensable naphthalene-containing polyimide by using reaction-induced crystallization. Eur Polym J. 2013;49:2334–43.
26. Puls J, Wilson SA, Hölter D. Degradation of cellulose acetate-based materials: a review. J Polym Environ. 2011;19:152–65.
27. Wang QW, Yoon KH, Min BG. Chemical and physical modification of poly(p-phenylene benzobisoxazole) polymers for improving properties of the PBO fibers. I. Ultraviolet-ageing resistance of PBO fibers with naphthalene moiety in polymer chain. Fiber Polym. 2015;16:1–7.
28. Braun JL, Kadla JF. Diffusion and saponification inside porous cellulose triacetate fibers. Biomacromolecules. 2005;6:152–60.
29. Nemr AE, Ragab S, Sikaily AE, Khaled A. Synthesis of cellulose triacetate from cotton cellulose by using NIS as a catalyst under mild reaction conditions. Carbohyd Polym. 2015;130:41–8.
30. Pushpamalar V, Langford SJ, Ahmad M, Lim YY. Optimization of reaction conditions for preparing carboxymethyl cellulose from sago waste. Carbohyd Polym. 2006;64:312–8.
31. Sun XF, Sun RC, Sun JX. Acetylation of sugarcane bagasse using NBS as a catalyst under mild reaction conditions for the production of oil sorption-active materials. Bioresource Techno. 2004;95:343–50.
32. Steinmeier H. Acetate manufacturing, process and technology. Macromol Symp. 2004;208:49–60.
33. Pan G, Du Z, Zhang C, Li C, Yang X. Synthesis, characterization, and properties of novel novolac epoxy resin containing naphthalene moiety. Polymer. 2007;48:3686–93.
34. Cao Y, Wu J, Meng T, Zhang J, He J, Li H, Zhang Y. Acetone-soluble cellulose acetates prepared by one-step homogeneous acetylation of cornhusk cellulose in an ionic liquid 1-allyl-3-methylimidazolium chloride (AmimCl). Carbohyd Polym. 2007;69:665–72.
35. Wang CS, Lee MC. Synthesis and modification of a naphthalene-containing trifunctional epoxy resin for electronic applications. J Appl Polym Sci. 1998;70:1907–21.
36. Ferguson J, Reeves LW, Schneider WG. Vapor absorption spectra and oscillator strengths of naphthalene, anthracene, and pyrene. Can J Chem. 1957;35:1117–36.
37. George GA, Morris GC. The intensity of absorption of naphthalene from 30,000 cm^{-1} to 53,000 cm^{-1}. J Mol Spectrosc. 1968;26:67–71.
38. Suto M, Wang X, Shan J, Lee LC. Quantitative photoabsorption and fluorescence spectroscopy of benzene, naphthalene, and some derivatives at 106–295 nm. J Quant Spectrosc Ra. 1992;48:79–89.
39. Moraes ACMD, Andrade PF, Faria AFD, Simões MB, Barros EB. Fabrication of transparent and ultraviolet shielding composite films based on graphene oxide and cellulose acetate. Carbohyd Polym. 2015;123:217–27.
40. Teranishi M, Okutsu W, Matsumoto N. Vapor deposition film for packing foodstuffs, has layer formed by acid-proof providing agent containing acid-proof providing resin component consisting of polyester resin and/or polyester polyurethane resin. EP Patent; 2005.